University of Nevada, Reno

Nevada Bureau of Mines and Geology Open-File Report 11-1

Comparison of Loss-Estimation Modeling Using HAZUS with Ground-Motion Input from ShakeMap versus Default Values

Jonathan G. Price[1], Gary Johnson[1], Glenn Biasi[2], Douglas Bausch[3], and Ivan G. Wong[4]

2011

This report, which is available as an online document at www.nbmg.unr.edu, documents a comparison of the Federal Emergency Management Agency's loss-estimation model, HAZUS, for earthquakes using two different ground-motion inputs: (1) the standard or default input using the epicenter, depth, and magnitude of an earthquake, which results in a simplified calculation of ground motions performed internally in HAZUS and (2) a user-supplied ShakeMap, which is created with a U.S. Geological Survey program that maps ground shaking. Except at small magnitudes (5.0, when the ShakeMap input yields significantly less loss than the standard input), the two approaches yield results that are mostly well within an order of magnitude of one another.

[1]Nevada Bureau of Mines and Geology
[2]Nevada Seismological Laboratory
[3]Federal Emergency Management Agency
[4]URS Corporation

Introduction

This report documents a comparison of HAZUS, the loss-estimation model developed by the Federal Emergency Management Agency (FEMA), for earthquakes using two different ground-motion inputs: (1) the standard or default input (the arbitrary event option) using the epicenter, depth, and magnitude of an earthquake, which results in a simplified calculation of ground motions performed internally in HAZUS (FEMA, 2003) and (2) a user-supplied ShakeMap, which is created with a U.S. Geological Survey (USGS) program that maps ground shaking (http://earthquake.usgs.gov/earthquakes/shakemap/).

FEMA's loss-estimation model for earthquakes, floods, and wind storms (HAZUS) is a valuable tool in emergency management, for mitigation, training, and emergency response. In Nevada, the results of HAZUS runs (see particularly Hess and dePolo, 2006; Price et al., 2007a, 2007b, and 2009) provided background information for the *State of Nevada Hazard Mitigation Plan – 2010*, which is available on line at http://www.nbmg.unr.edu/nhmpc/NV_plan_2010/index.html, and its 2007 predecessor. The Nevada Bureau of Mines and Geology (NBMG) and the Nevada Division of Emergency Management (NDEM) have incorporated HAZUS results in building several regional and statewide training exercises for emergency response and recovery.

NBMG has used HAZUS immediately after an earthquake to transmit information about the likely severity of the event to the NDEM Chief, who advises the Governor regarding the decision whether to ask for federal assistance. The memo to NDEM contains the following cautionary note:

> "**The results of this computer simulation are not actual damage or casualty figures.** They can be off by a factor of 10 (an estimate of 100 could, in reality, be between 10 and 1,000). These numbers should only be used to ascertain the likely severity of the event and assist the State in making decisions regarding deployment of resources to assist local governments in responding to the event. These results have helped other states to decide whether to request a Presidential Declaration of Disaster."

Even with this order-of-magnitude uncertainty (Price et al., 2010), the HAZUS results are useful in the first few hours or days after a significant earthquake.

Using the arbitrary event option in its default or standard mode, HAZUS uses the epicenter, depth, and magnitude supplied by the user to calculate earthquake ground motions using a simplified approach. This arbitrary event option can result in significant differences in ground motions when compared to an actual event. Following NBMG protocols after an actual earthquake, we use the first epicenter, depth, and magnitude that has been checked by a seismologist at the USGS's National Earthquake Information Center (NEIC), which operates 24/7. The Nevada Seismological Laboratory (NSL) at the University of Nevada, Reno works closely with the USGS to provide real-time seismic information including epicenters, depths, and magnitudes. In some instances, as was the case with the 21 February 2008 moment magnitude (**M**) 6.0 earthquake near Wells, Nevada, NSL may be incorporating data from more seismic stations than are routinely available to the USGS.

ShakeMap, which incorporates actual measurements of ground shaking from strong motion stations, provides a much more accurate portrayal of the actual ground shaking in an event than what is modeled by HAZUS in its default mode, if there are a sufficient number of stations to create an accurate map covering the impacted area. ShakeMap version 3.5 and standard ShakeMap ground-motion modules were used in this study. For earthquakes of **M** 5.3 and larger, NSL uses the ShakeMap "HAZUS PGV" module, which is based on the ground-motion prediction model of Boore et al. (1997). In contrast, when using the arbitrary event option with epicenter, depth, and magnitude as input, HAZUS uses a combination of weighted ground-motion models (FEMA, 2003), including 20% for Boore et al. (1997) for earthquakes in extensional areas of the western United States. For earthquakes of **M** less than 5.3, ShakeMap is configured to use the ShakeMap "Small" module, in which Boore et al. (1997) was adjusted using data from southern California. The NSL version of ShakeMap also includes a model layer for site conditions based on topographic slope, which incorporates measurements of shear-wave velocity rather than assuming a default classification.

Efforts are under way by the California Office of Emergency Management to automate the use of ShakeMap output as input for HAZUS. Currently, a ShakeMap output file has to be added during the HAZUS input protocols.

Beginning in the fall of 2010, the USGS began incorporating estimates of economic loss and deaths, in order-of-magnitude ranges, into its Prompt Assessment of Global Earthquakes for Response (PAGER) alerts (http://earthquake.usgs.gov/earthquakes/pager/) and began to include this information for domestic as well as foreign earthquakes. These automated USGS PAGER alerts should serve as useful checks of future HAZUS results shortly after an earthquake.

Methods

For this comparison, we used the latest version of HAZUS available to us as of August 2010–HAZUS MR4, release 9.2.0. Since our work preparing HAZUS scenarios for 38 communities in Nevada (Price et al., 2009), there have been some updates to HAZUS. The NBMG's version of HAZUS incorporates an adjustment to the centroids of population for some of the larger census tracts, for which Douglas Bausch helped move the location of the population from the geographic centroid of the polygon to approximately the center of mass of the population in the census tract.

For comparisons in this report, we used 10 earthquakes, five each (**M** 5.0, 5.5, 6.0, 6.5, and 7.0) for the cities of Reno and Carson City. The earthquake locations and magnitudes are the same as reported by Price et al. (2009)–earthquakes on the closest Quaternary fault to the center of the city (dePolo, 2008). For both cities, the faults are within 2 km of the city centers: the north end of the Mount Rose fault zone in Reno and the Carson City fault. According to dePolo et al. (1997), both faults are capable of **M** 7 earthquakes: a **M** 7.1 ± 0.3 for the Mount Rose fault zone and **M** 6.8 ± 0.3 for the Carson City fault.

The HAZUS model with the arbitrary event option assumes the default NEHRP site class D for stiff soil (shear-wave velocity of 180 to 360 m/sec). The NSL version of ShakeMap includes a user-supplied V_S30 (the average shear-wave velocity in the top 30 m) grid estimated using topographic slope (Wald and Allen, 2007), from which NEHRP site classifications are derived. For the Reno area, V_S30 values range from approximately 310 m/sec to 360 m/sec. Therefore both approaches use NEHRP site class D for most of the populated region.

When using HAZUS with the arbitrary event option, the fault is assumed to have a north-south-trending strike and vertical dip. Variation in dip, which is not normally determined in the first few minutes or hours after an earthquake, had little effect on HAZUS results in tests documented by Price et al. (2010).

ShakeMap models were generated in two modes. The first set uses only the epicenters, depths, and magnitudes as with the arbitrary event option, but with no information about the fault length or orientation. In this mode, having no information about the fault strike or dip, ShakeMap internally adjusts ground motions slightly upward using a geometric adjustment designed to compensate for the lack of information. The ShakeMap ground-motion input for HAZUS from this mode parallels what would be available in the first few minutes to possibly hours after a real earthquake. For four of the scenarios (**M** 5.0 and 7.0 for each city), we developed ShakeMaps using the "finite-fault" mode with fault location, size, orientation, and dip identical to those for the corresponding arbitrary events. These ShakeMap finite-fault inputs consisted of north-striking vertical fault patches centered on the hypocenters and scaled to the lengths used in the arbitrary event option (taken from the regressions for rupture length versus magnitude proposed by Wells and Coppersmith, 1994).

Results

We have chosen five outputs from the HAZUS runs to compare the three sets of ground-motion input–total economic loss, the number of buildings suffering major (extensive to complete) damage, the number of people needing public shelter, the number of people needing hospitalization, and the number of fatalities. These outputs are summarized in table 1. Note that table 1 has hyperlinks to the individual, 20-page HAZUS global summary reports for these runs.

Table 1. Comparison of results using different ground-motion inputs for HAZUS.

	Magnitude	Economic Loss ($ million)	Number of buildings with major Damage	Number of people needing public shelter	Number of people needing hospital care	Fatalities at 2 p.m.
Carson City using arbitrary event option	5.0	**83**	**57**	**16**	**2**	**0**
	5.5	**221**	**255**	**58**	**8**	**1**
	6.0	**630**	**1,430**	**241**	**49**	**12**
	6.5	**1,518**	**3,568**	**584**	**170**	**43**
	7.0	**3,733**	**7,795**	**1,746**	**530**	**140**
using ShakeMap without fault orientation	5.0	**5**	**0**	**0**	**0**	**0**
	5.5	**81**	**7**	**2**	**1**	**0**
	6.0	**229**	**188**	**51**	**4**	**1**
	6.5	**568**	**1,065**	**200**	**33**	**7**
	7.0	**1,454**	**2,944**	**502**	**166**	**43**
ShakeMap with fault orientation	5.0	**5**	**0**	**0**	**0**	**0**
	7.0	**1,803**	**3,593**	**573**	**207**	**53**
Reno using arbitrary event option	5.0	**300**	**123**	**82**	**8**	**1**
	5.5	**750**	**517**	**276**	**25**	**5**
	6.0	**1,935**	**3,109**	**1,224**	**165**	**41**
	6.5	**3,837**	**7,821**	**2,586**	**541**	**143**
	7.0	**5,837**	**12,466**	**3,832**	**987**	**266**
using ShakeMap without fault orientation	5.0	**16**	**0**	**0**	**0**	**0**
	5.5	**326**	**17**	**15**	**2**	**0**
	6.0	**921**	**426**	**268**	**20**	**2**
	6.5	**2,014**	**2,276**	**1,215**	**141**	**32**
	7.0	**4,450**	**7,014**	**3,157**	**702**	**189**
ShakeMap with fault orientation	5.0	**15**	**0**	**0**	**0**	**0**
	7.0	**4,189**	**8,192**	**2,917**	**597**	**158**

Sets of figures illustrate the differences in these results. Figures 1 and 2 are plots of estimated total economic loss versus magnitude for Reno and Carson City, respectively. Figures 3 and 4 are plots of estimated numbers of buildings damaged in Reno and Carson City, respectively.

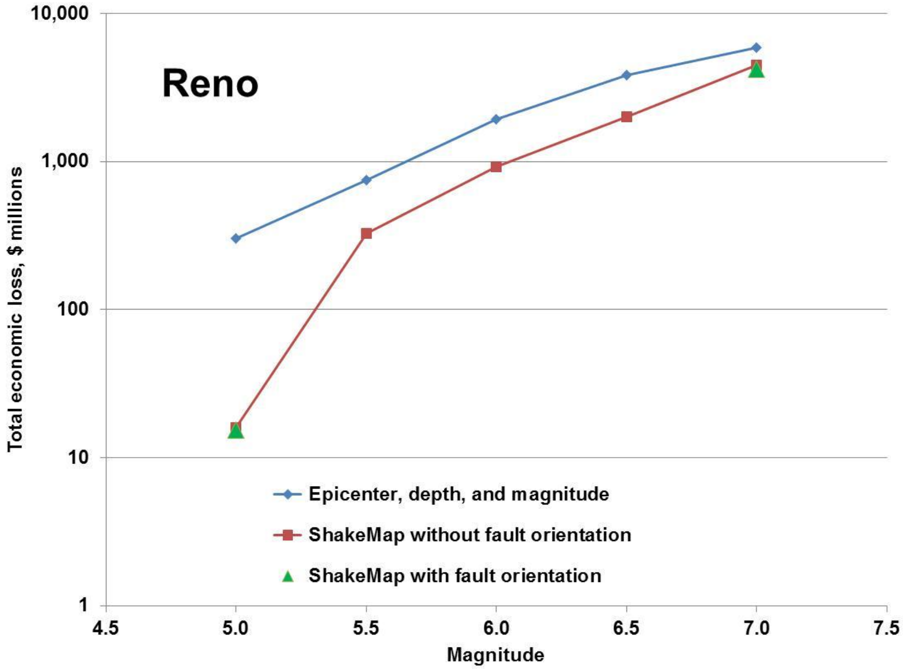

Figure 1. Comparison of estimates of total economic loss for Reno.

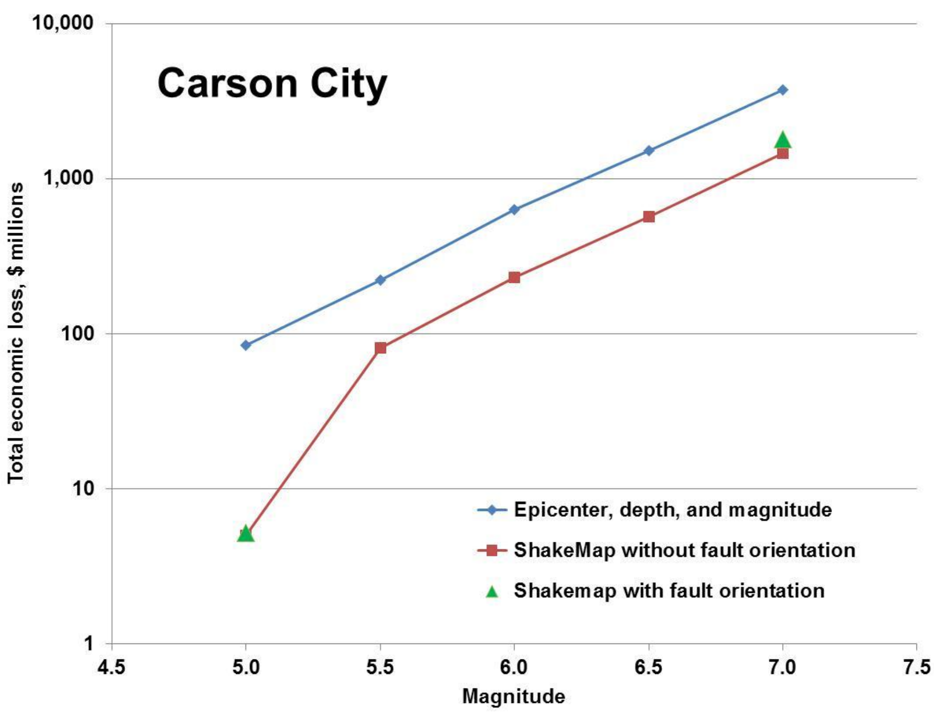

Figure 2. Comparison of estimates of total economic loss for Carson City.

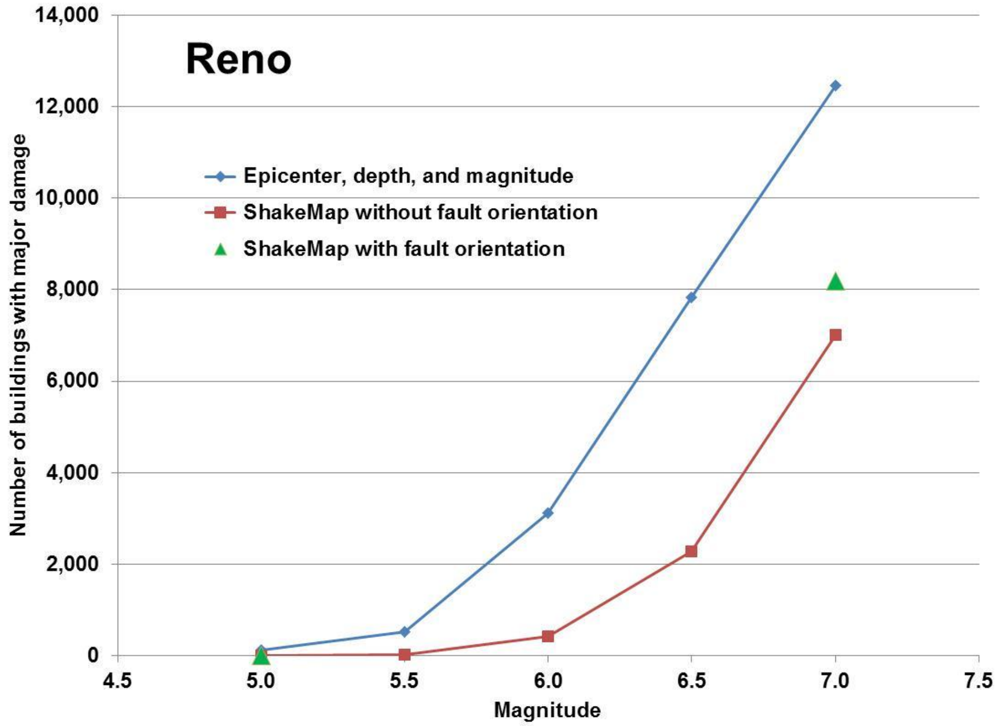

Figure 3. Comparison of estimates of number of buildings damaged in Reno.

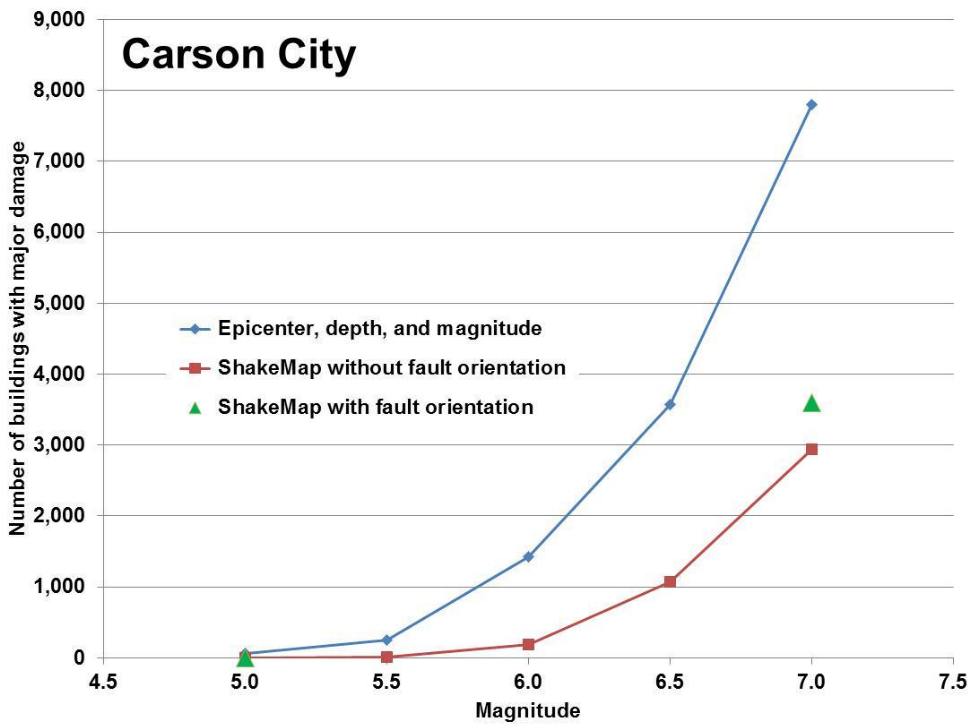

Figure 4. Comparison of estimates of number of buildings damaged in Carson City.

Figures 5 to 8 compare the ground motions (0.3 second spectral acceleration) from ShakeMap assuming a north-south fault orientation with those from the arbitrary event option for the **M** 7.0 earthquake scenarios. The ground motions are shown by census tract.

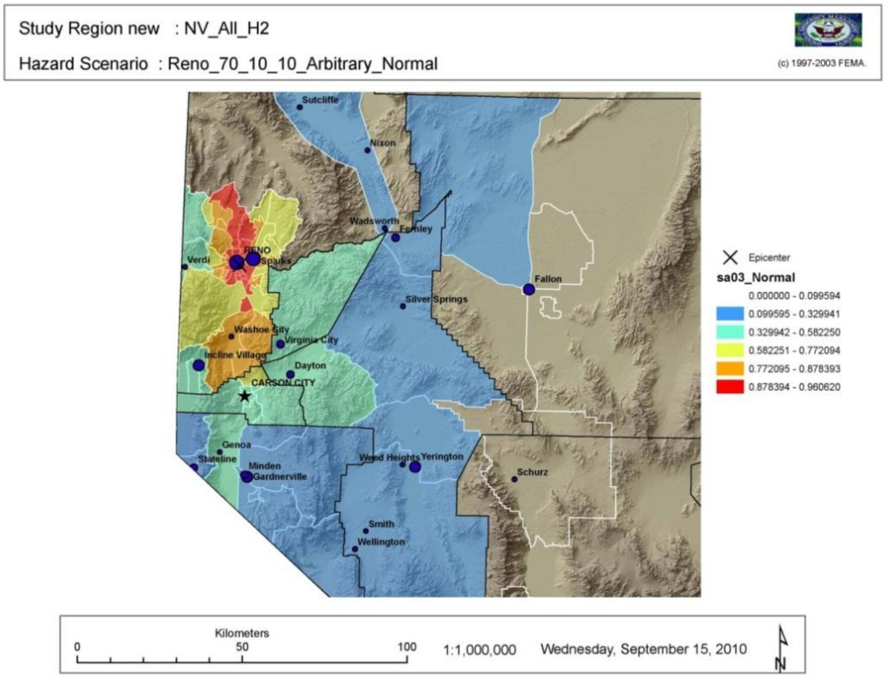

Figure 5. Ground shaking, by census tract, for **M** 7.0 earthquake in Reno, using the arbitrary event option (colors correspond to the ranges in 0.3 sec spectral acceleration measured as a fraction of gravity). Compare with figure 6.

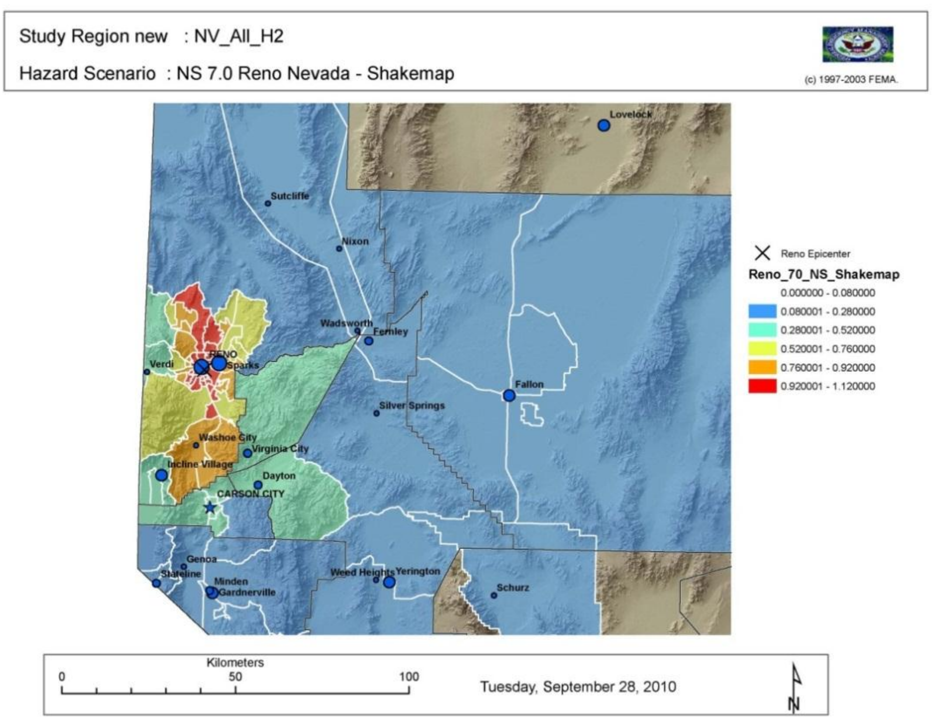

Figure 6. Ground shaking, by census tract, for **M** 7.0 earthquake in Reno, using ShakeMap with a north-south fault orientation as input (colors correspond to the ranges in 0.3 sec spectral acceleration measured as a fraction of gravity). Compare with figure 5.

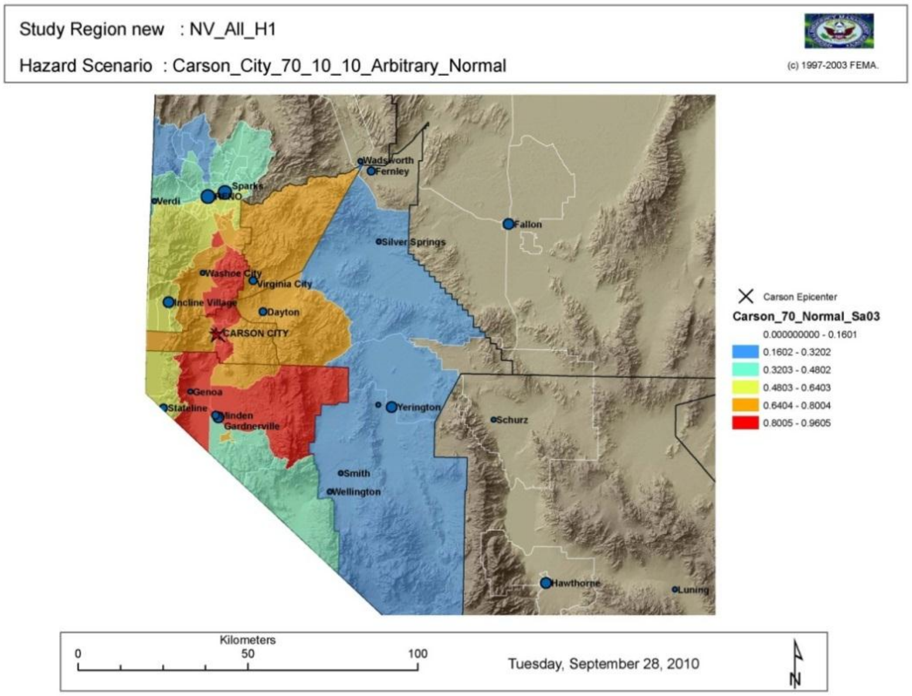

Figure 7. Ground shaking, by census tract, for **M** 7.0 earthquake in Carson City, using the arbitrary event option (colors correspond to the ranges in 0.3 sec spectral acceleration measured as a fraction of gravity). Compare with figure 8.

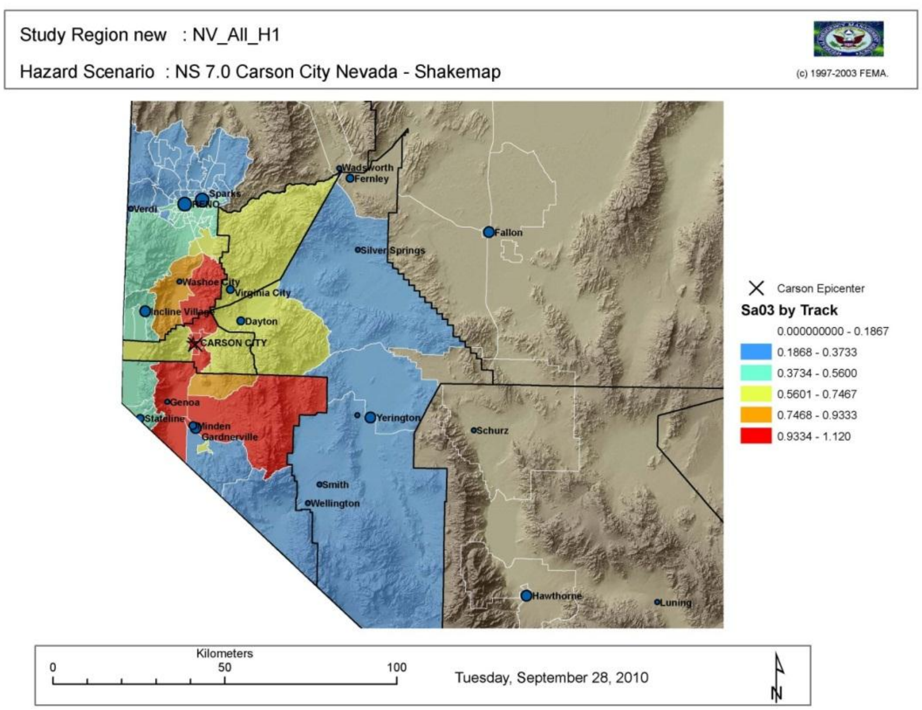

Figure 8. Ground shaking, by census tract, for **M** 7.0 earthquake in Carson City, using ShakeMap with a north-south fault orientation as input (colors correspond to the ranges in 0.3 sec spectral acceleration measured as a fraction of gravity). Compare with figure 7.

Discussion

Except at small magnitudes (in our comparison, at **M** 5.0, when the ShakeMap input yields significantly less loss than the standard input), the two approaches are mostly well within an order of magnitude of one another. Given other uncertainties in HAZUS (Price et al., 2010), either approach provides useful information.

The differences between HAZUS runs using the arbitrary event option versus ShakeMap input are likely the result of differences in fragility functions and ground-motion prediction approaches (attenuation models). HAZUS uses a more recent set of fragility functions with a ShakeMap input than with the arbitrary event option. Kircher (2006) analyzed a suite of actual earthquakes and recommended the fragility functions that are used in the current version of HAZUS with ShakeMap input (case B in table 2). In its default mode, HAZUS uses its original fragility functions (case A in table 2). HAZUS using the arbitrary event option can be tricked into using the same fragility functions as ShakeMap by converting the ground motions generated by the default HAZUS run into a ShakeMap for input (case C in table 2). The fact that cases B and C are nearly identical suggests that differences in fragility functions explain most of the observed differences between outputs using ShakeMap versus the arbitrary event option for the **M** 5.0 earthquake.

Table 2. Comparison of results using different fragility functions for the **M** 5.0 earthquake near Carson City.

	Magnitude	Economic Loss ($ million)	Number of buildings with major damage	Number of people needing public shelter	Number of people needing hospital care	Fatalities at 2 p.m.
A. Default (using arbitrary event option)	5.0	83	57	16	2	0
B. ShakeMap (with or without fault orientation)	5.0	5	0	0	0	0
C. HAZUS (using arbitrary event option, but same fragility functions as ShakeMap)	5.0	3	0	0	0	0

For the **M** 7.0 earthquake, however, differences in fragility functions do not account for all the differences in damage numbers when comparing ShakeMap input with the arbitrary event input. As with the **M** 5.0 event, HAZUS with the arbitrary event and its original fragility functions (case A in table 3) yields higher damage numbers than using the fragility functions recommended by Kircher (2006) (case C in table 3). These latter numbers are nonetheless higher than those generated with the ShakeMap input (case B in table 3).

Table 3. Comparison of results using different fragility functions for the **M** 7.0 earthquake near Carson City.

	Magnitude	Economic Loss ($ million)	Number of buildings with major damage	Number of people needing public shelter	Number of people needing hospital care	Fatalities at 2 p.m.
A. Using arbitrary event option	7.0	3,733	7,795	1,746	530	140
B. Using ShakeMap with fault orientation	7.0	1,803	3,593	573	207	53
C. Using arbitrary event with fragility functions as with ShakeMap	7.0	2,826	6,339	1,088	364	95

Figures 9 through 32 illustrate the differences in the ground motions that are used in the two approaches. Because contour intervals are slightly different on the corresponding maps, comparisons are difficult to make. For most examples, however, the arbitrary event option predicts larger areas with higher ground motions than those using ShakeMap with a north-south fault orientation. The ground motions using ShakeMap without a fault orientation have even smaller areas of strong ground shaking than either of the other approaches.

The differences are most apparent for the **M** 5.0 events (figures 27-32). Using the peak ground acceleration figures in table 4, ground shaking is 32 to 37% higher when using the arbitrary event option than when using ShakeMap for the **M** 5.0 events, whereas it is only 8 to 10% higher for the **M** 7.0 events. These differences likely contribute to the higher losses obtained using HAZUS with the arbitrary event option than with ShakeMap input.

Table 4. Comparison of peak ground accelerations (fraction of the acceleration due to gravity).

	Reno **M** 5.0	Carson City **M** 5.0	Reno **M** 7.0	Carson City **M** 7.0
A. Default (using arbitrary event option)	0.1919	0.1848	0.4628	0.4524
B. ShakeMap (with or without fault orientation)	0.14	0.14	0.42	0.42

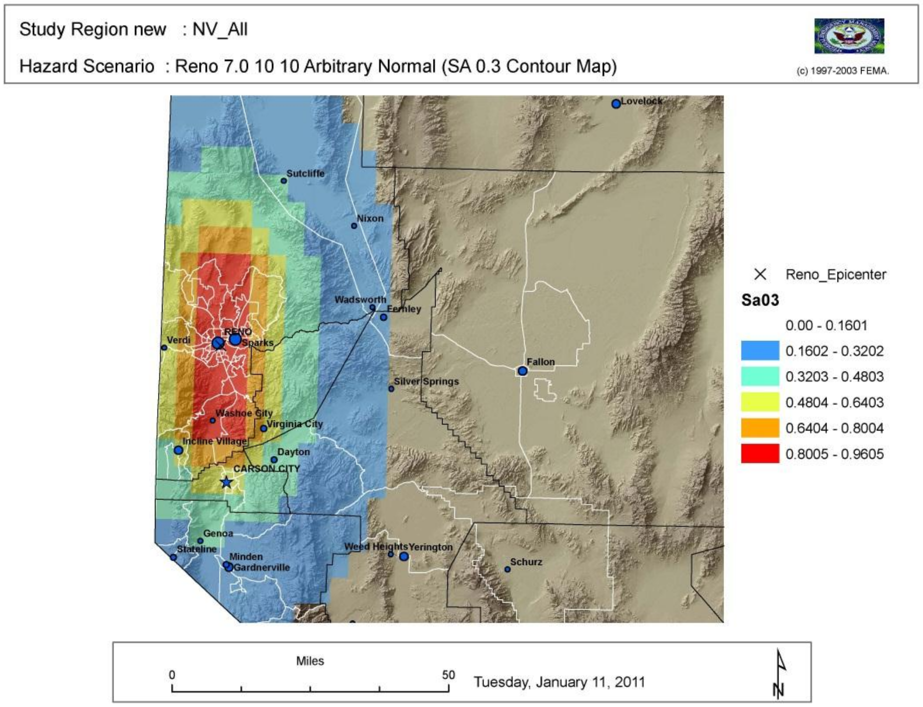

Figure 9. Ground shaking, contoured, for **M** 7.0 earthquake in Reno, using the arbitrary event option (colors correspond to the ranges in 0.3 sec spectral acceleration measured as a fraction of gravity). Compare with figures 10 and 11.

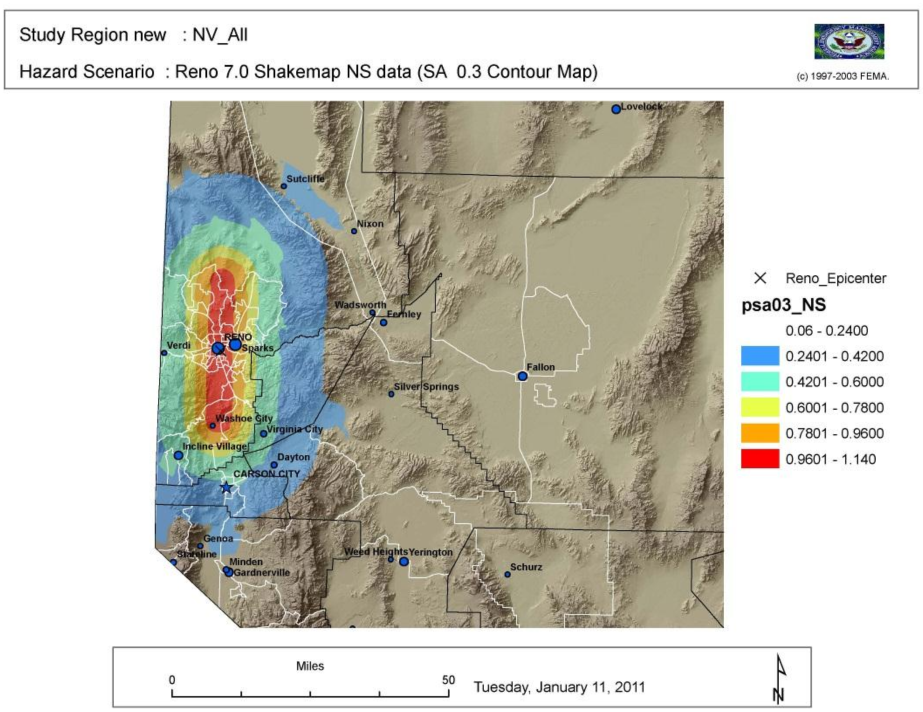

Figure 10. Ground shaking, contoured, for **M** 7.0 earthquake in Reno, using ShakeMap with a north-south fault orientation as input (colors correspond to the ranges in 0.3 sec spectral acceleration measured as a fraction of gravity). Compare with figures 9 and 11.

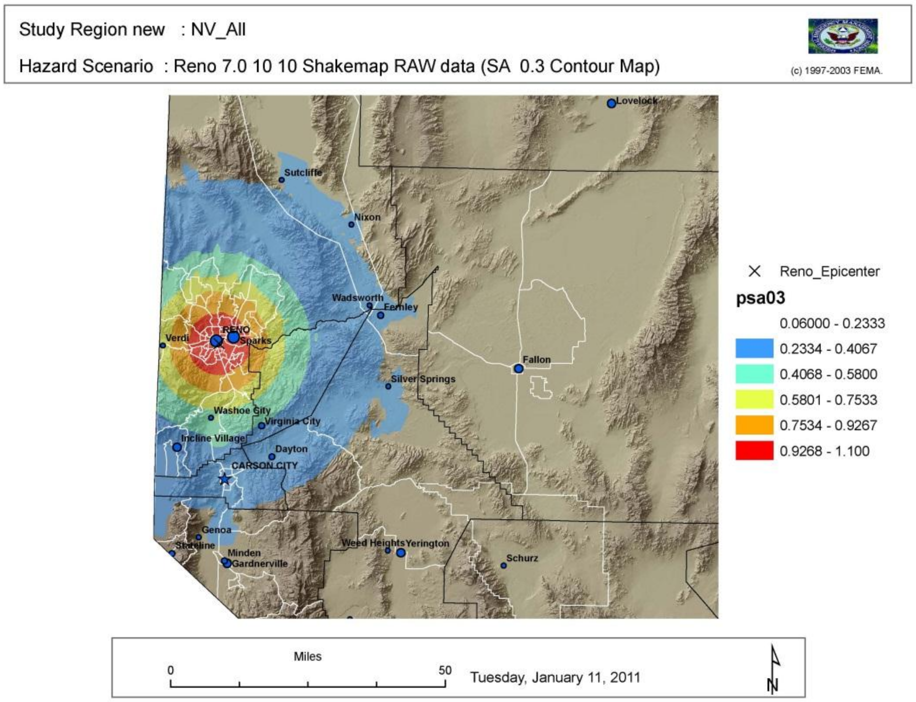

Figure 11. Ground shaking, contoured, for **M** 7.0 earthquake in Reno, using ShakeMap without a fault orientation (colors correspond to the ranges in 0.3 sec spectral acceleration measured as a fraction of gravity). Compare with figures 9 and 10.

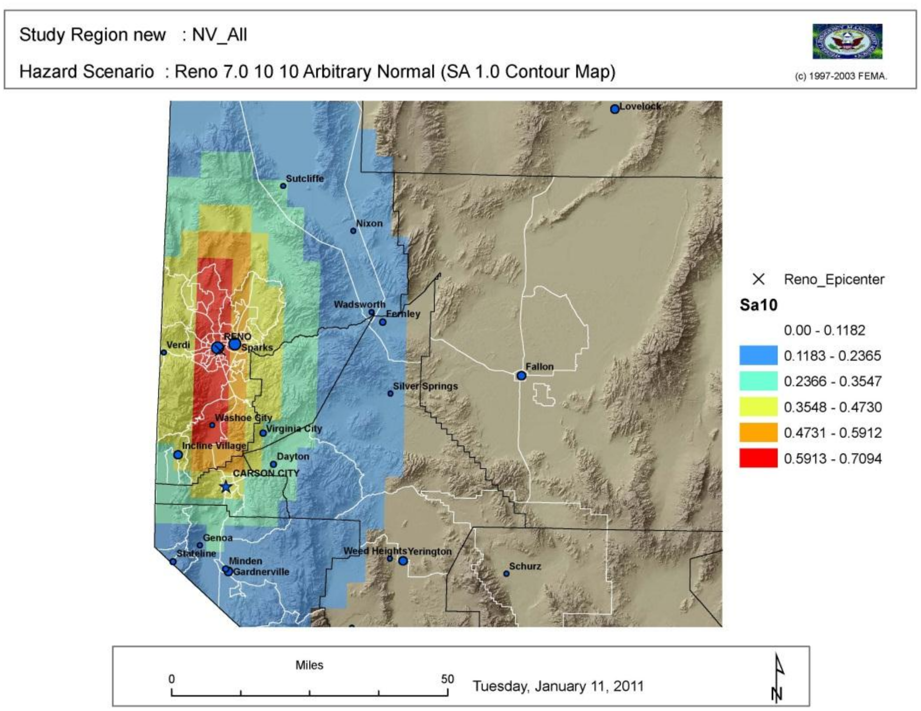

Figure 12. Ground shaking, contoured, for **M** 7.0 earthquake in Reno, using the arbitrary event option (colors correspond to the ranges in 1.0 sec spectral acceleration measured as a fraction of gravity). Compare with figures 13 and 14.

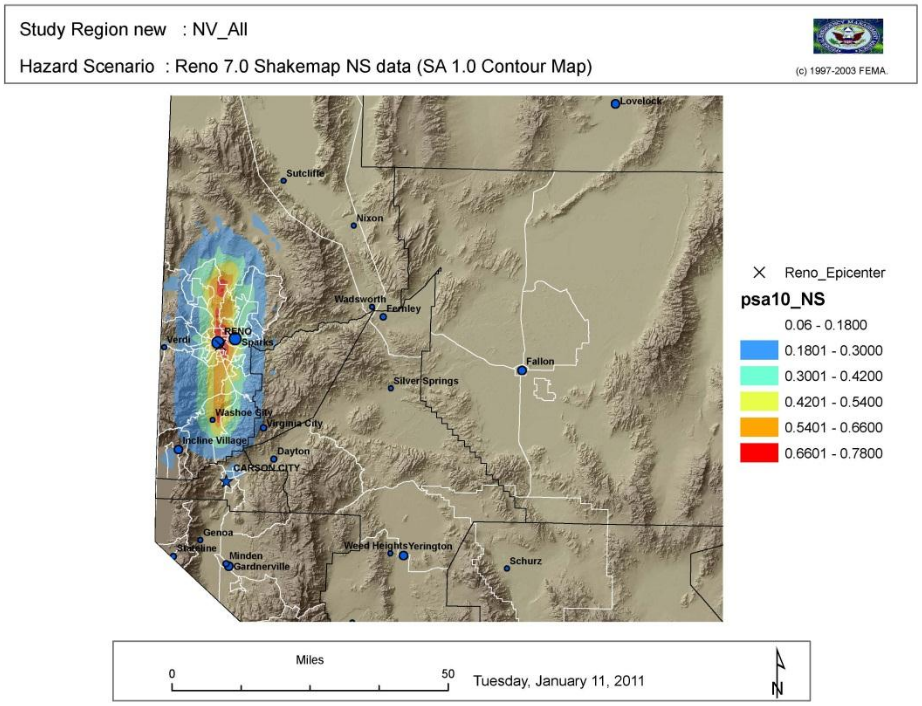

Figure 13. Ground shaking, contoured, for **M** 7.0 earthquake in Reno, using ShakeMap with a north-south fault orientation as input (colors correspond to the ranges in 1.0 sec spectral acceleration measured as a fraction of gravity). Compare with figures 12 and 14.

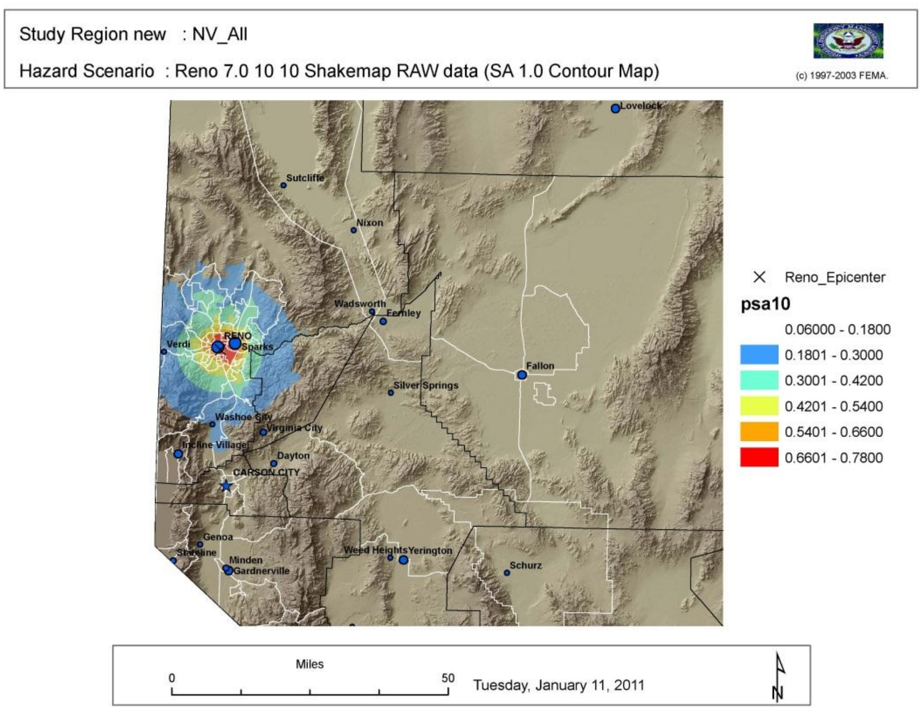

Figure 14. Ground shaking, contoured, for **M** 7.0 earthquake in Reno, using ShakeMap without a fault orientation (colors correspond to the ranges in 1.0 sec spectral acceleration measured as a fraction of gravity). Compare with figures 12 and 13.

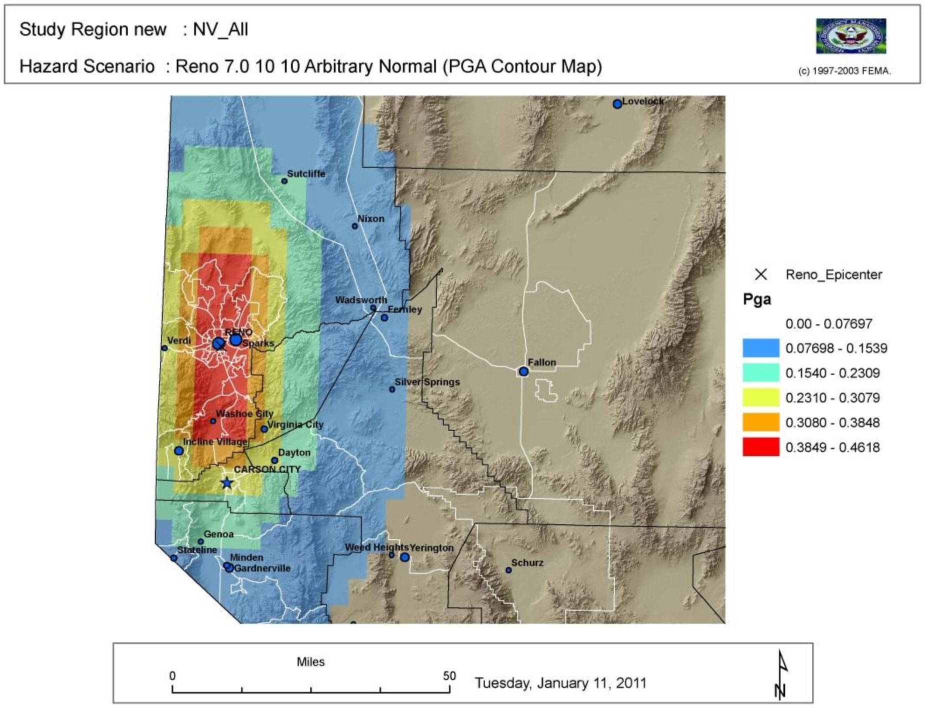

Figure 15. Ground shaking, contoured, for **M** 7.0 earthquake in Reno, using the arbitrary event option (colors correspond to the ranges in peak ground acceleration measured as a fraction of gravity). Compare with figures 16 and 17.

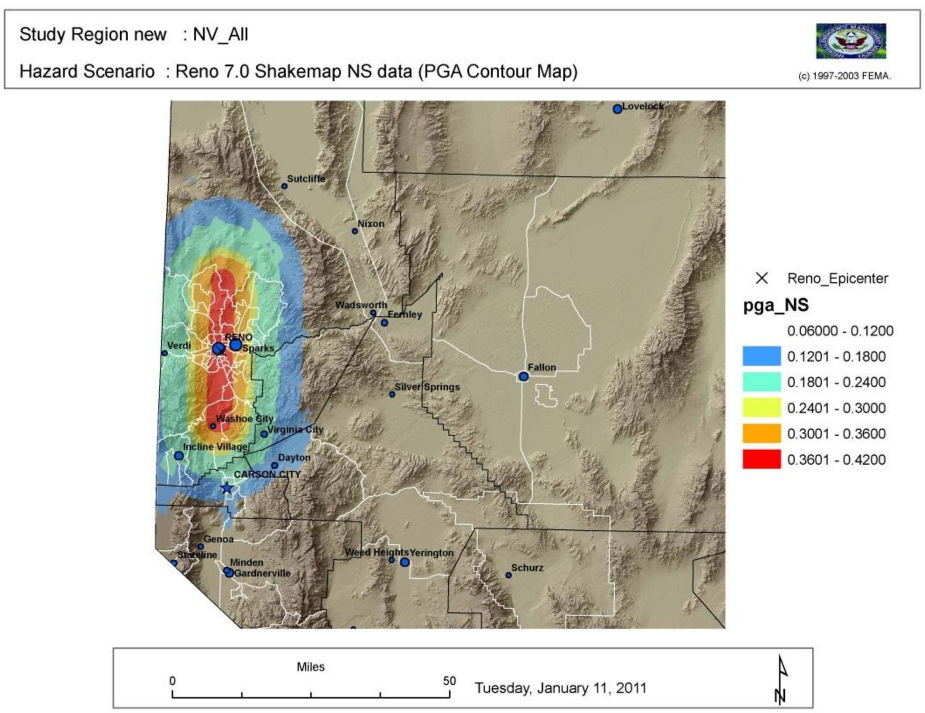

Figure 16. Ground shaking, contoured, for **M** 7.0 earthquake in Reno, using ShakeMap with a north-south fault orientation as input (colors correspond to the ranges in peak ground acceleration measured as a fraction of gravity). Compare with figures 15 and 17.

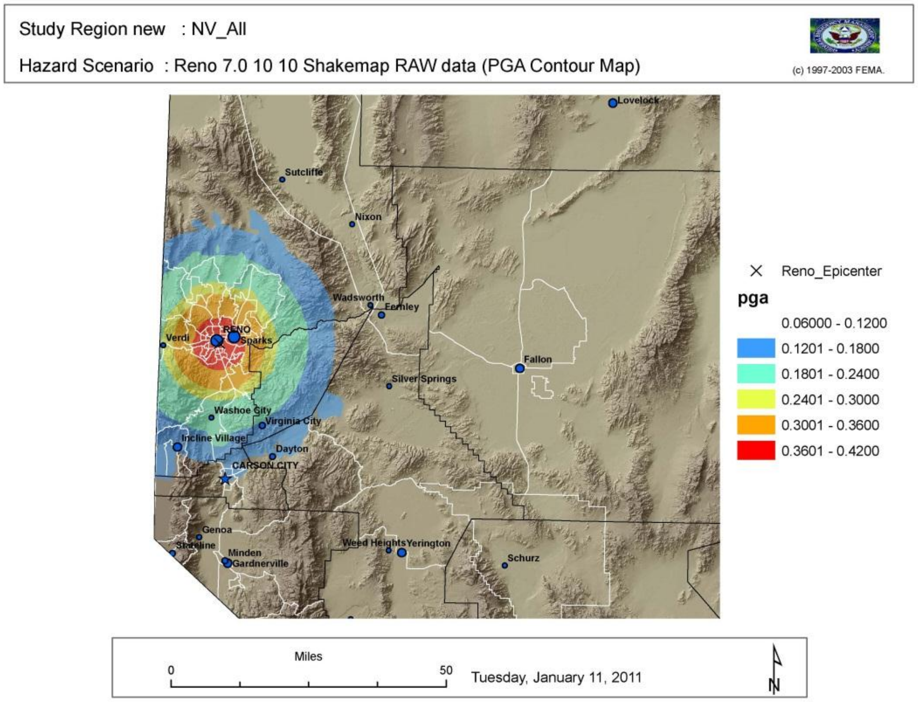

Figure 17. Ground shaking, contoured, for **M** 7.0 earthquake in Reno, using ShakeMap without a fault orientation (colors correspond to the ranges in peak ground acceleration measured as a fraction of gravity). Compare with figures 15 and 16.

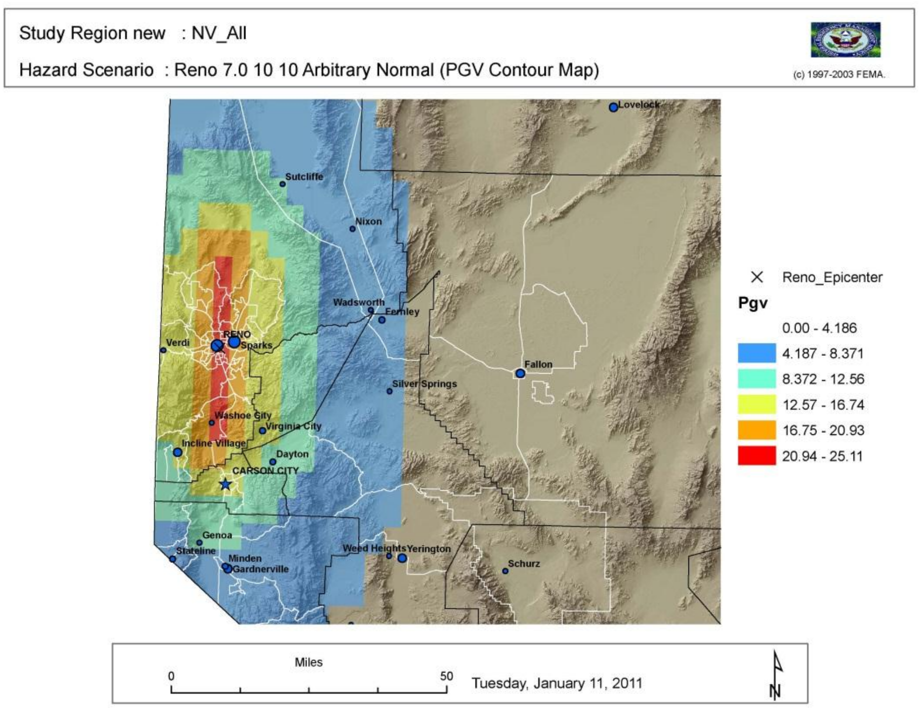

Figure 18. Ground shaking, contoured, for **M** 7.0 earthquake in Reno, using the arbitrary event option (colors correspond to the ranges in peak ground velocity in cm/sec). Compare with figures 19 and 20.

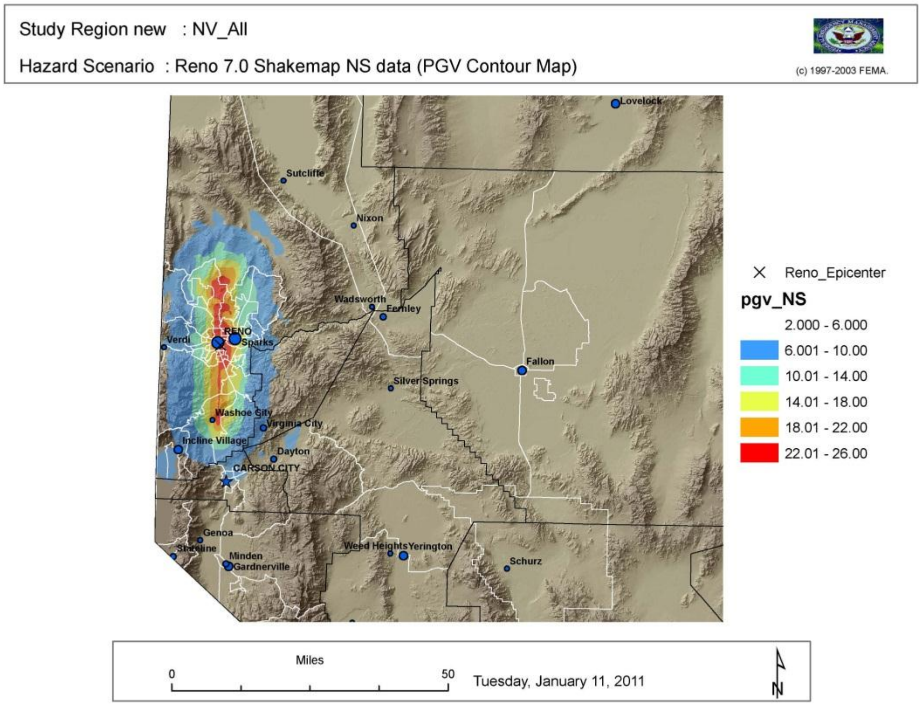

Figure 19. Ground shaking, contoured, for **M** 7.0 earthquake in Reno, using ShakeMap with a north-south fault orientation as input (colors correspond to the ranges in peak ground velocity in cm/sec). Compare with figures 18 and 20.

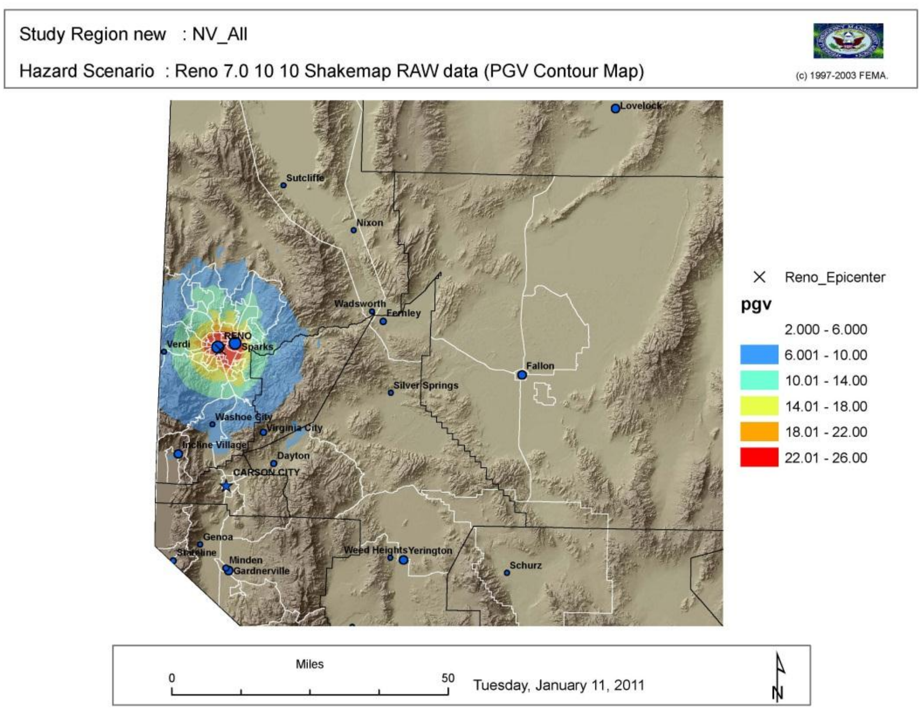

Figure 20. Ground shaking, contoured, for **M** 7.0 earthquake in Reno, using ShakeMap without a fault orientation (colors correspond to the peak ground velocity in cm/sec). Compare with figures 18 and 19.

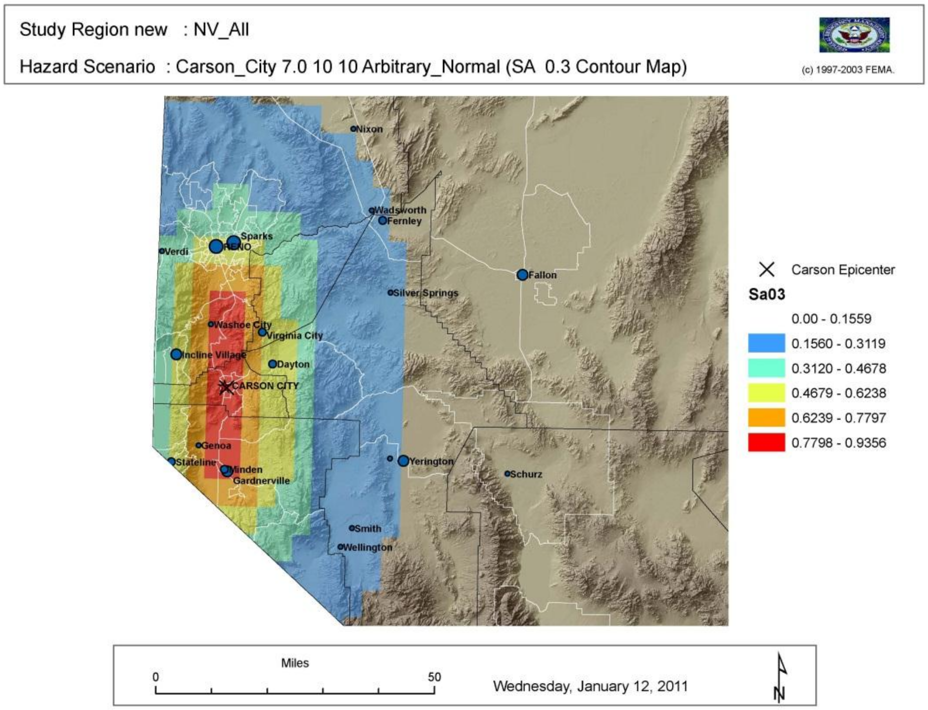

Figure 21. Ground shaking, contoured, for **M** 7.0 earthquake in Carson City, using the arbitrary event option (colors correspond to the ranges in 0.3 sec spectral acceleration measured as a fraction of gravity). Compare with figure 22.

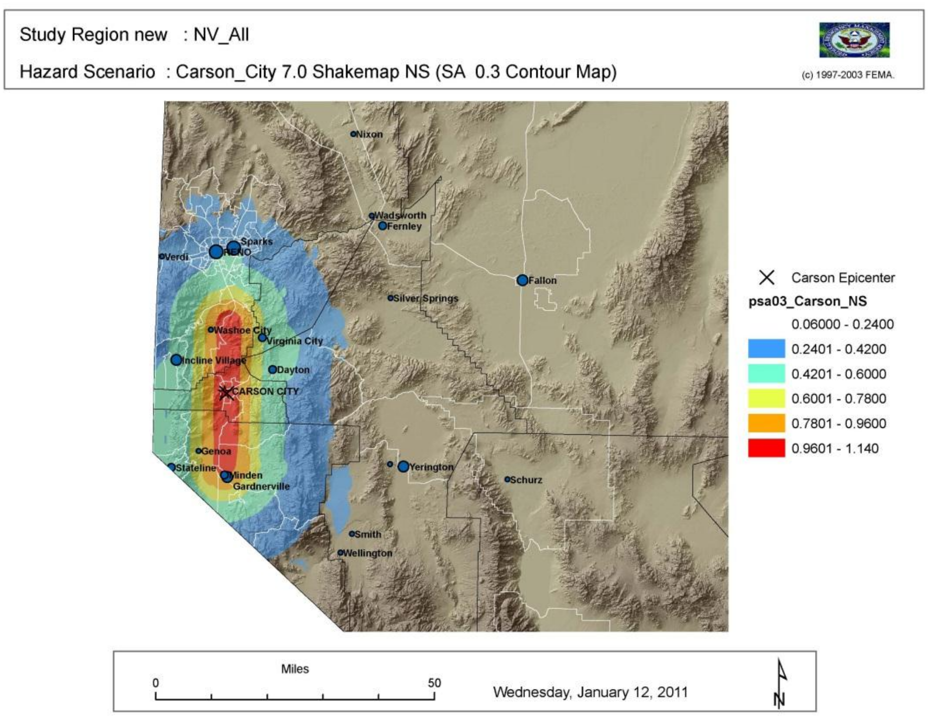

Figure 22. Ground shaking, contoured, for **M** 7.0 earthquake in Carson City, using ShakeMap with a north-south fault orientation as input (colors correspond to the ranges in 0.3 sec spectral acceleration measured as a fraction of gravity). Compare with figure 21.

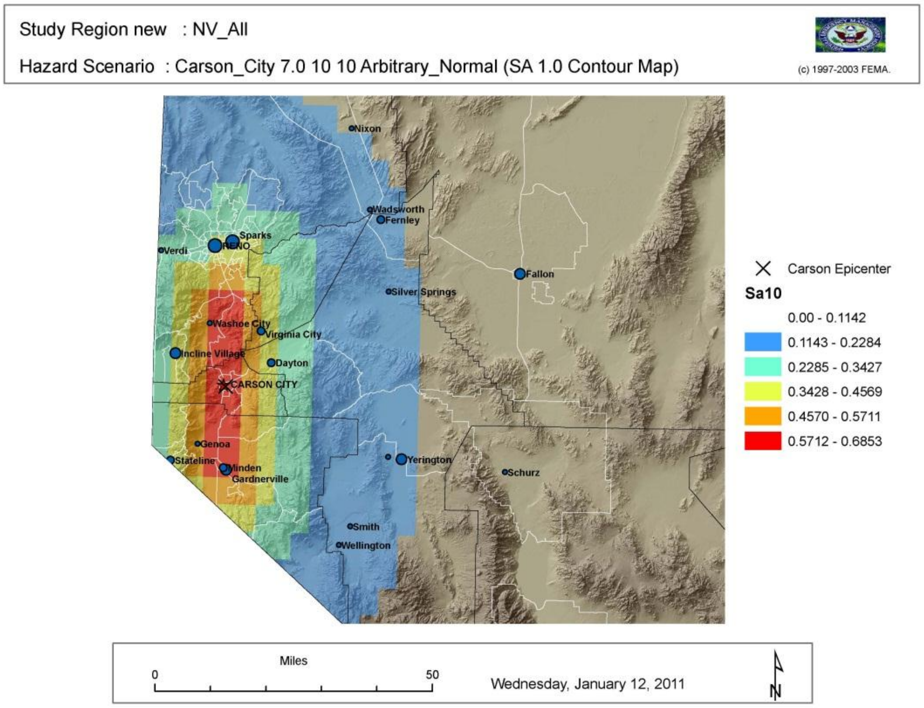

Figure 23. Ground shaking, contoured, for **M** 7.0 earthquake in Carson City, using the arbitrary event option (colors correspond to the ranges in 1.0 sec spectral acceleration measured as a fraction of gravity). Compare with figure 24.

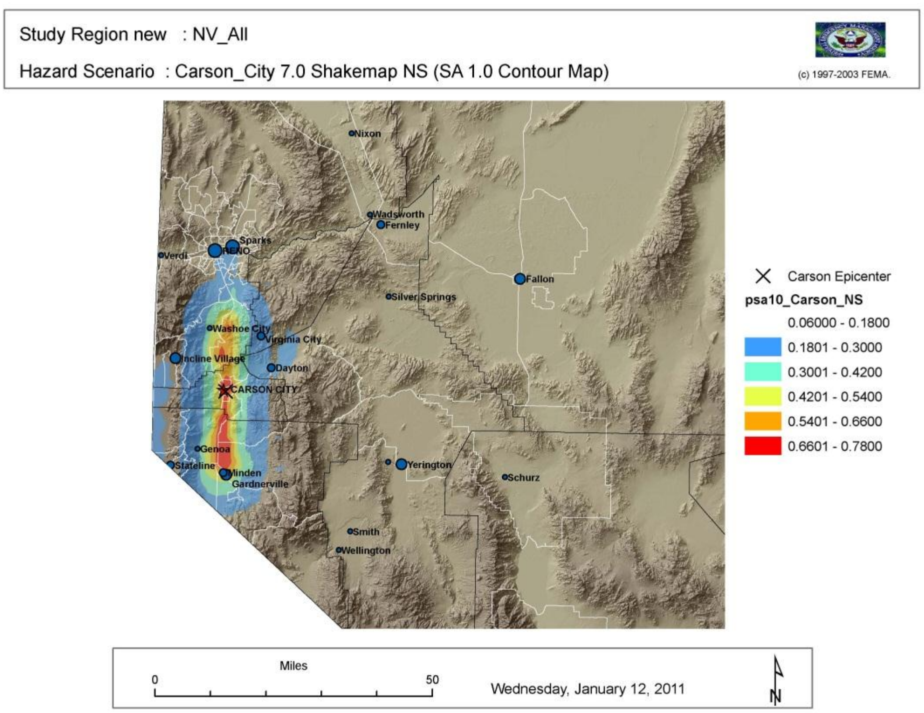

Figure 24. Ground shaking, contoured, for **M** 7.0 earthquake in Carson City, using ShakeMap with a north-south fault orientation as input (colors correspond to the ranges in 1.0 sec spectral acceleration measured as a fraction of gravity). Compare with figure 23.

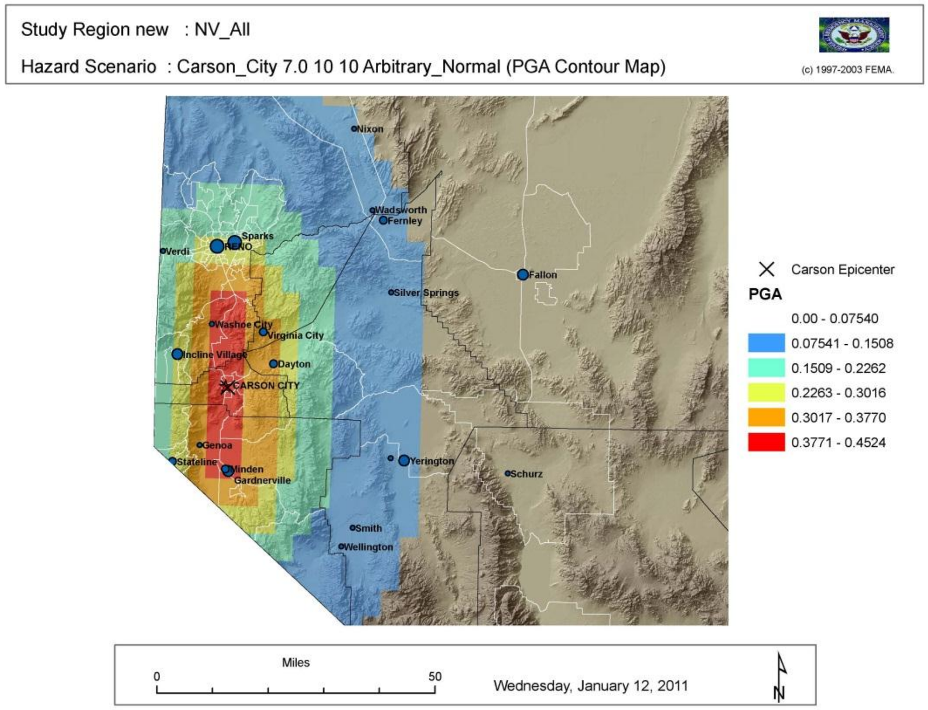

Figure 25. Ground shaking, contoured, for **M** 7.0 earthquake in Carson City, using the arbitrary event option (colors correspond to the ranges in peak ground acceleration measured as a fraction of gravity). Compare with figure 26.

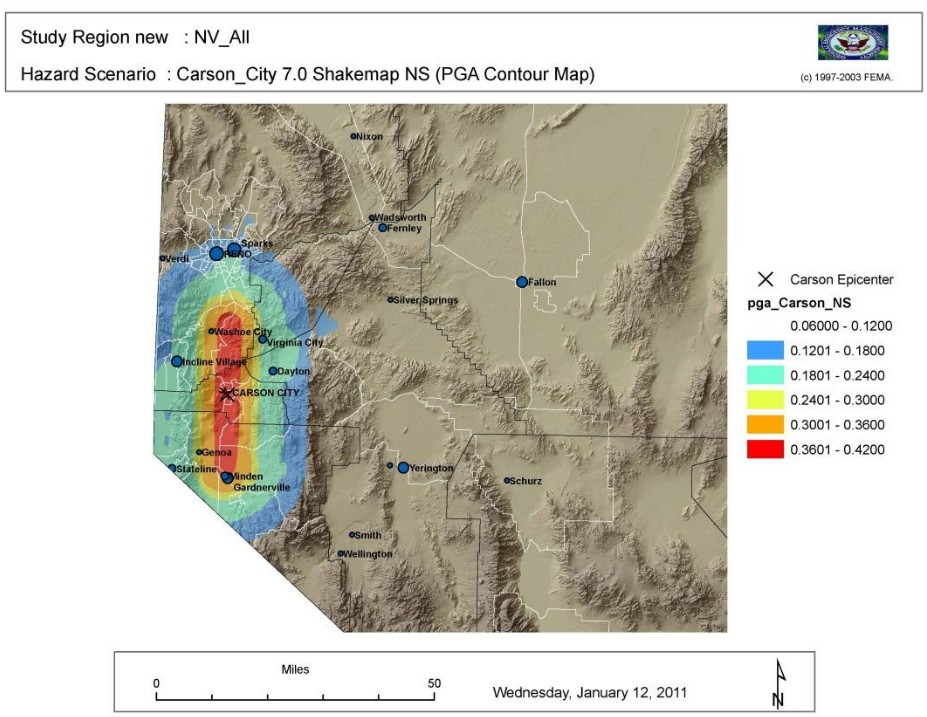

Figure 26. Ground shaking, contoured, for **M** 7.0 earthquake in Carson City, using ShakeMap with a north-south fault orientation as input (colors correspond to the ranges in peak ground acceleration measured as a fraction of gravity). Compare with figure 25.

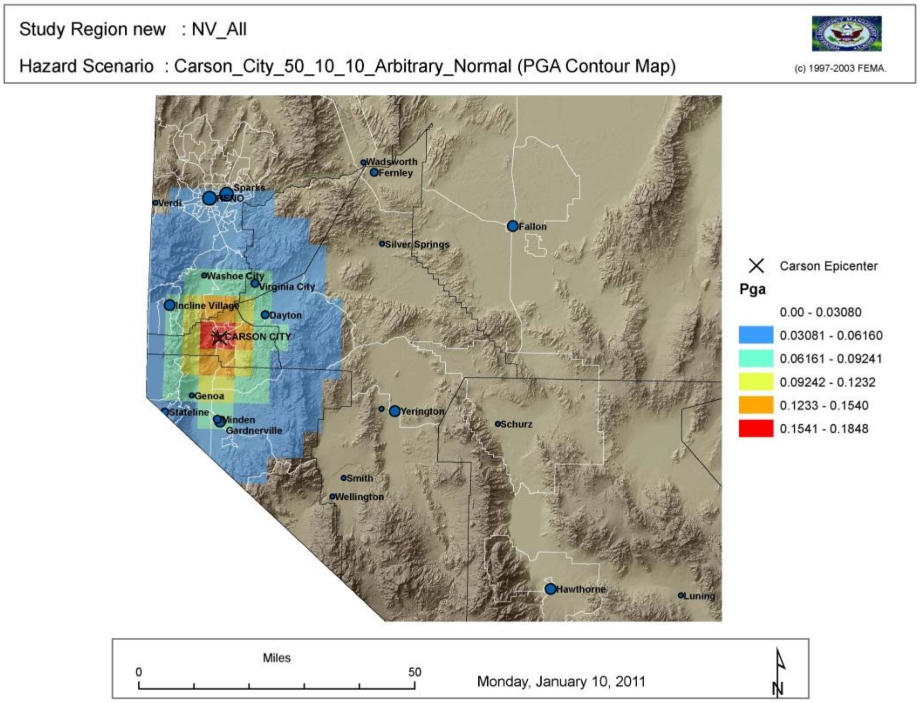

Figure 27. Ground shaking, contoured, for **M** 5.0 earthquake in Carson City, using the arbitrary event option (colors correspond to the ranges in peak ground acceleration measured as a fraction of gravity). Compare with figures 28 and 29.

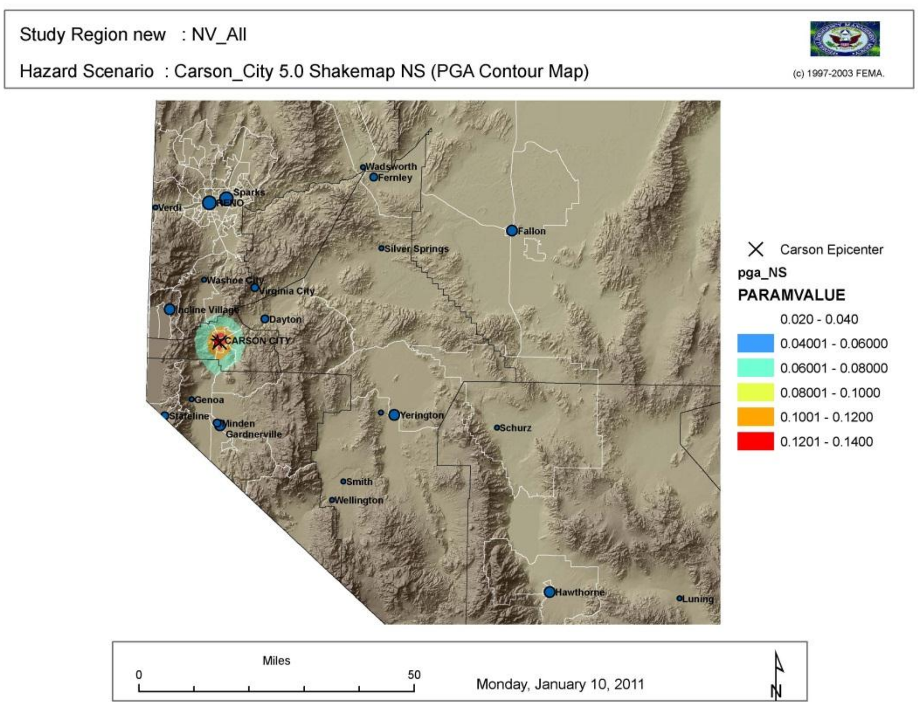

Figure 28. Ground shaking, contoured, for **M** 5.0 earthquake in Carson City, using ShakeMap with a north-south fault orientation as input (colors correspond to the ranges in peak ground acceleration measured as a fraction of gravity). Compare with figures 27 and 29.

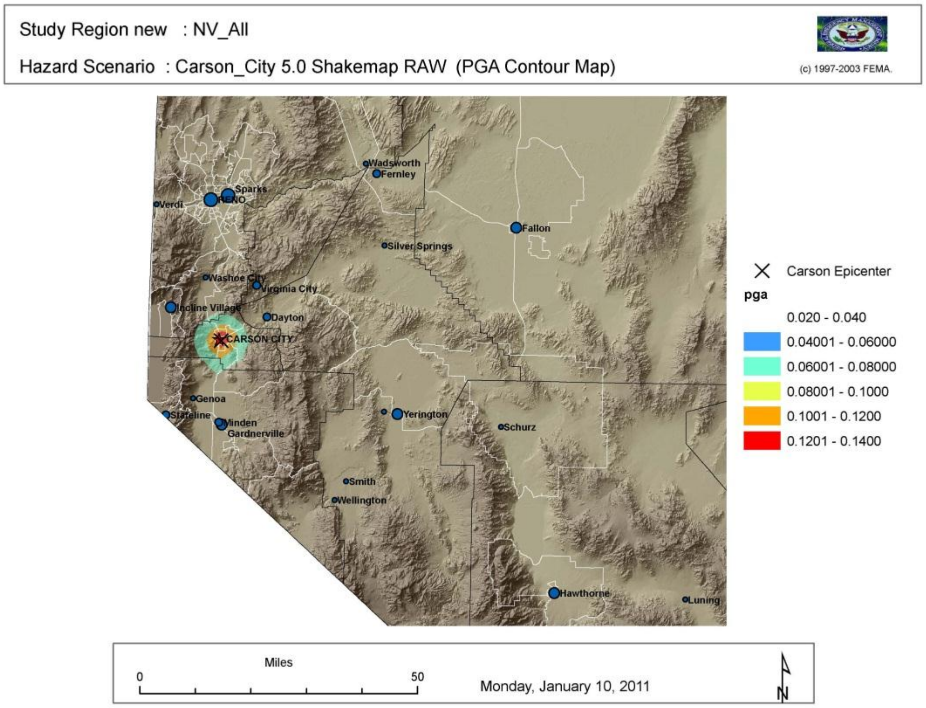

Figure 29. Ground shaking, contoured, for **M** 5.0 earthquake in Carson City, using ShakeMap without a fault orientation as input (colors correspond to the ranges in peak ground acceleration measured as a fraction of gravity). Compare with figures 27 and 29.

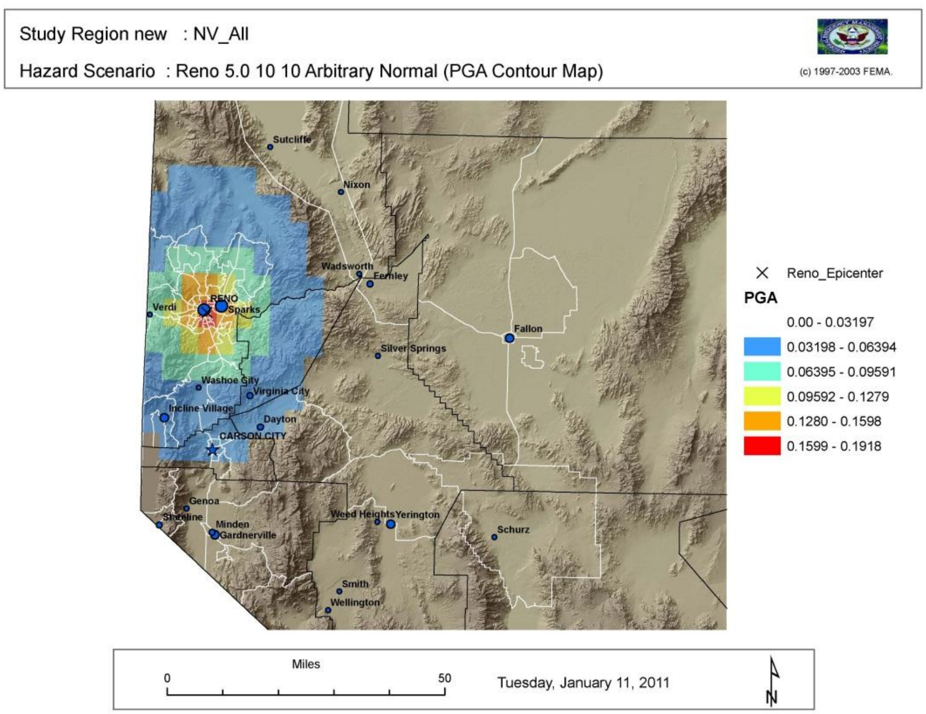

Figure 30. Ground shaking, contoured, for **M** 5.0 earthquake in Reno, using the arbitrary event option (colors correspond to the ranges in peak ground acceleration measured as a fraction of gravity). Compare with figures 31 and 32.

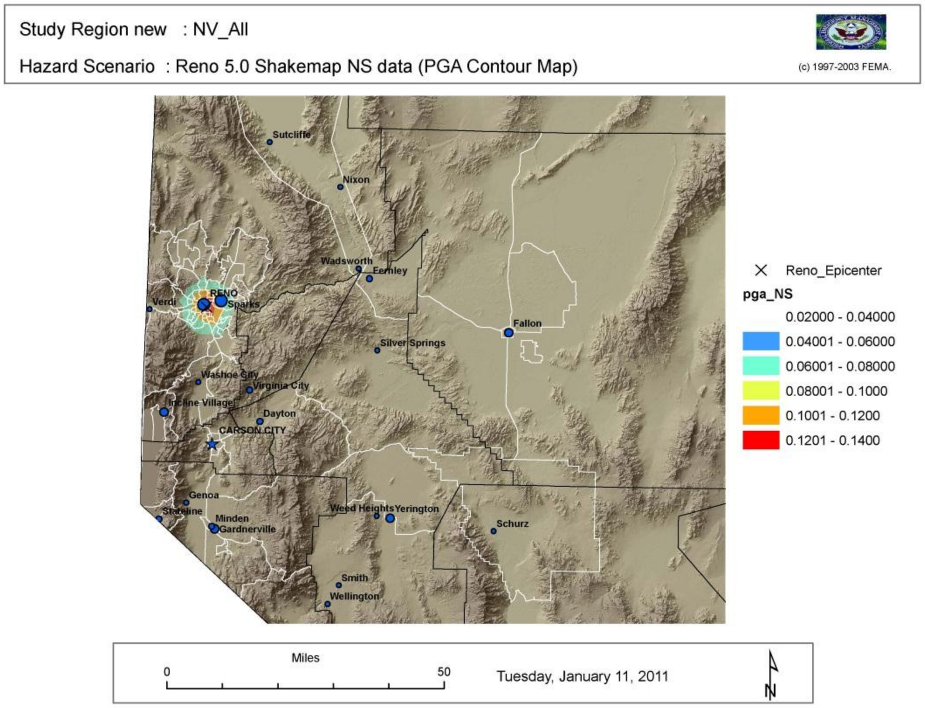

Figure 31. Ground shaking, contoured, for **M** 5.0 earthquake in Reno, using ShakeMap with a north-south fault orientation as input (colors correspond to the ranges in peak ground acceleration measured as a fraction of gravity). Compare with figures 30 and 32.

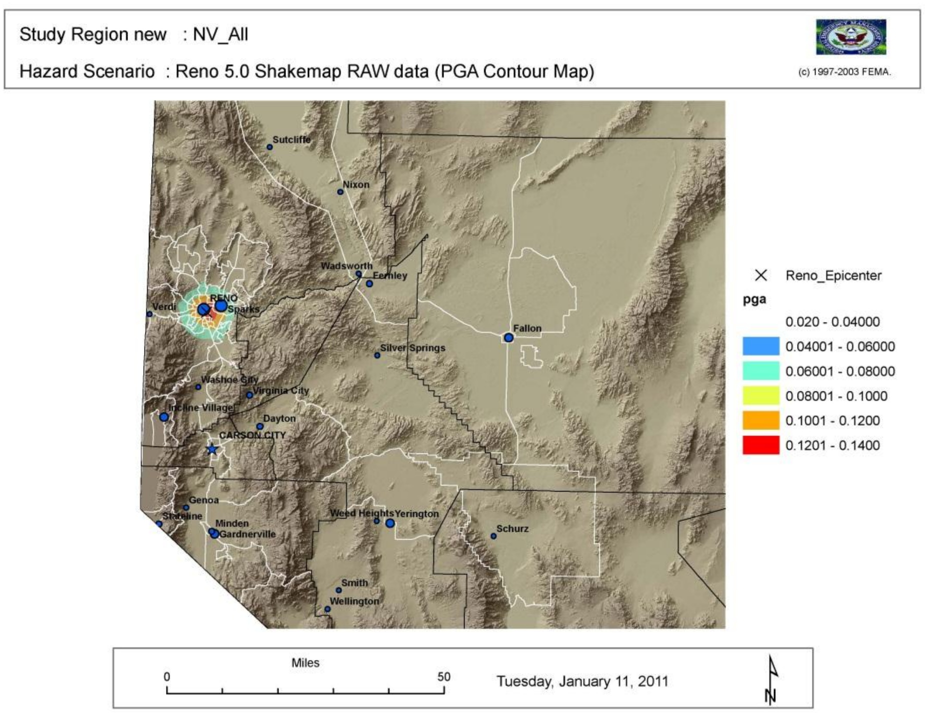

Figure 32. Ground shaking, contoured, for **M** 5.0 earthquake in Reno, using ShakeMap without a fault orientation as input (colors correspond to the ranges in peak ground acceleration measured as a fraction of gravity). Compare with figures 30 and 31.

Conclusions and Recommendations

Loss estimates from HAZUS using ground motions calculated internally using the default or arbitrary event option (inputting epicenter, depth, and magnitude and assuming a north-south fault orientation with a vertical dip) are higher than those calculated by HAZUS using ShakeMap as input, probably for two main reasons: different fragility functions and different ground-motion prediction approaches. The two approaches yield results that are mostly well within an order of magnitude of one another. The order-of-magnitude caution should continue to be included in communicating a summary of HAZUS results to NDEM immediately after an earthquake.

The fragility functions used by HAZUS when modeling losses with ShakeMap input are preferred over those used with the arbitrary event option. HAZUS should be updated, such that these newer, preferred fragility functions are used as the default for running HAZUS with the arbitrary event option.

ShakeMap provides more accurate information about ground shaking than that derived from HAZUS using the arbitrary event option because, in a real earthquake, ShakeMap incorporates actual measurements of ground motion. Unfortunately, we still have too few strong motion stations, even in and near our urban areas in Nevada, to create ShakeMaps without heavily relying on ground-motion prediction models to estimate likely shaking across the affected area. Nonetheless, we should be using the ShakeMap that is automatically created after an earthquake as input for HAZUS. Efforts are under way between NSL and NBMG to automate inclusion of ShakeMap into HAZUS runs. Once the automation has been implemented and checked, NSL and NBMG will advise NDEM of changes in procedures for producing the HAZUS run to be used in communicating information to NDEM immediately after an earthquake. Before summarizing results and forwarding them to NDEM, NBMG should check the results against the USGS PAGER estimates of total economic loss and number of fatalities for that earthquake and against previously run HAZUS scenarios for earthquakes near 38 communities throughout Nevada (Price et al., 2009).

Acknowledgments

This work was supported by the Nevada Bureau of Mines and Geology, the Nevada Seismological Laboratory, and a grant from the Federal Emergency Management Agency. We thank both FEMA and the USGS for their interest in refining the tools needed for reducing risks from earthquakes. We also thank URS Corporation for their efforts, made possible through FEMA funding, to encourage the use of ShakeMaps as input for HAZUS.

Disclaimer

The information in this report should be considered preliminary. It has not been thoroughly edited or peer reviewed.

References

Ballard, C.M., Johnson, G., and Hastings, J.T., 2009, Nevada statewide HAZUS database update: Nevada Bureau of Mines and Geology Open-File Report 09-7, 3 p., with links to updated files, http://www.nbmg.unr.edu/dox/of097/of097.pdf.

Boore, D. M., Joyner, W.B., and Fumal, T.E., 1997, Equations for estimating horizontal response spectra and peak acceleration from western North American earthquake: a summary of recent work: Seismological Research Letters, v. 68, pp. 128-153.

dePolo, C.M., Quaternary faults in Nevada: Nevada Bureau of Mines and Geology Map 167, 1:1,000,000 scale.

dePolo, C.M., Anderson, J.G., dePolo, D.M., and Price, J.G., 1997, Earthquake occurrence in the Reno-Carson City urban corridor: Seismological Research Letters, v. 68, no. 3, p. 401-412.

Federal Emergency Management Agency, 2003, Multi-hazard loss estimation methodology, earthquake model, HAZUS-MH MR4 technical manual, development by the Department of Homeland Security, Emergency Preparedness and Response Directorate under a contract with the National Institute of Building Sciences, Washington, D.C., 16 chapters, and Multi-hazard loss estimation methodology, earthquake module, HAZUS MH MR4 user manual, 11 chapters. Electronic document, available at http://www.fema.gov/library/viewRecord.do?fromSearch=fromsearch&id=3731 and http://www.fema.gov/library/viewRecord.do?fromSearch=fromsearch&id=3732.

Hess, R., and dePolo, C.M., 2006, Loss-estimation modeling of earthquake scenarios for each county in Nevada using HAZUS-MH: Nevada Bureau of Mines and Geology Open-File Report 06-1, 517 p., http://www.nbmg.unr.edu/dox/of061/of061.htm.

Kircher, C.A., Whitman, R.V., and Holmes, W.T., 2006, HAZUS earthquake loss estimation methods: Natural Hazards Review, May 2006, p. 45-59.

Price, J.G., Hastings, J.T., and Arritt, C.M., 2007a, Assessment of risks and vulnerability to earthquake hazards in Nevada: Nevada Bureau of Mines and Geology Open-File Report 07-1, 8 p., with links to plates, http://www.nbmg.unr.edu/dox/of071.pdf.

Price, J.G., Hastings, J.T., and Arritt, C.M., 2007b, Assessment of risks and vulnerability to flood hazards in Nevada: Nevada Bureau of Mines and Geology Open-File Report 07-2, 6 p., with links to plates, http://www.nbmg.unr.edu/dox/of072.pdf.

Price, J.G., Hastings, J.T., Goar, L.D., Armeno, H., Johnson, G., dePolo, C.M., Hess, R.H., and Ballard, C.M., 2010, Sensitivity analysis of loss-estimation modeling using uncertainties in earthquake parameters: Environmental and Engineering Geoscience, v. 16, no. 4, p. 357-367.

Price, J.G., Johnson, G., Ballard, C.M., Armeno, H., Seeley, I., Goar, L.D., dePolo, C.M., and Hastings, J.T., 2009, Estimated losses from earthquakes near Nevada communities: Nevada Bureau of Mines and Geology Open-File Report 09-8, 46 p., with links to 485 20-page HAZUS summary reports, http://www.nbmg.unr.edu/dox/of098/Scenarios/OpenFileReport09-8.pdf.

Wald, D. J., and T. I. Allen, 2007, Topographic slope as a proxy for seismic site conditions and amplification, Bulletin of the Seismological Society of America, v. 97, no. 5, p. 1379–1395.

Wells, D.L. and Coppersmith, K.J., 1994, New empirical relationships among magnitde, rupture length, rupture width, rupture area, and surface displacement: Bulletin of the Seismological Society of America, v. 4, no. 4, p.974-1002.